PAPER

Identification of the normal and abnormal glow discharge modes in a neon-xenon gas mixture at low pressure

View the article online for updates and enhancements.

Identification of the normal and abnormal glow discharge modes in a neon-xenon gas mixture at low pressure

B HECHELEF and A BOUCHIKHI

University of Saïda, Faculty of Technology, Department of Electrical Engineering, Saïda 20000, Algeria

E-mail: bouchikhiabdelaziz1@yahoo.fr

Abstract

In this paper, we focused on the identification of the normal and abnormal glow discharge modes in a neon-xenon gas mixture at low pressure. We considered four gas mixtures: 90%Ne-10%Xe, 80%Ne-20%Xe, 70%Ne-30%Xe and 50%Ne-50%Xe at 1.5 Torr. The range of the gap voltage is 150–500 V. A one-dimensional fluid model with multiple species was used in this work, and the metastable state of the atoms as well as the radiation effects were integrated into the model too. The input data changed for each percentage in the gas mixture, and was calculated by BOLSIG+ software. The parameters of particle transport and their rate coefficients strictly depend on the mean electron energy. The results show that the neon ion density is negligible compared to the xenon ion density, mostly in the case of 50%Ne-50%Xe.

Keywords: gas mixtures, Boltzmann's equation, Poisson's equation, Blanc's law, two-order fluid model

(Some figures may appear in colour only in the online journal)

1. Introduction

Glow discharge technology [1–6] is an important domain in the microelectronic industry, such as in etching or the deposition of thin solid films, as well as analytical spectroscopy for metallic and sputtering treatment. This technology is used in a lot of pure and mixed gases, but the material technologies which are used in the experimental setup vary from one to another, mostly in the cathode material, which directly influences the current–voltage characteristics. To give some results on the electric discharge, in this paper we propose the study of a neon-xenon DC glow discharge at low pressure with a high percentage of gas in the mixture. By utilizing a fluid model we can find the electrical and energetic characteristics in each mixture, but the problem is related to the type and the percentage of gas in each one. To give the best results using a fluid model, which are in good agreement with the experimental results, it is necessary to know several conditions.

In the research papers [7–10], we find that the electron energy distribution function (EEDF) can be Maxwellian at a very low pressure, and is related to the type of gas. The EEDF

is non-Maxwellian for a threshold pressure value, and is again related to the type of gas. Determining the percentage of gas in the mixture is related to the ion mass.

Experiments on the gas mixture have been carried out extensively. For example, the addition of H_2 in a Ne-Xe mixture was studied by Wei *et al* [11], showing an increasing current present in the discharge. Panchenko *et al* [12] studied the glow discharge in low-pressure excilamps, showing the effect of spontaneous radiation and the effect of halides in mixtures of inert gases, which generated the excited molecules $KrCl^*$, $XeCl^*$, and XeF^*. Hassouba and Mehanna [13] studied a N_2-H_2 gas mixture DC glow discharge at different pressures and electrode separations using a Langmuir single probe. They showed that the electron energy distribution function has a Maxwellian distribution in the positive column, and is a non-Maxwellian form in the cathode fall and negative glow regions.

The objective of this paper is to identify normal and abnormal glow discharge modes at low pressure in 90%Ne-10%Xe, 80%Ne-20%Xe, 70%Ne-30%Xe and 50%Ne-50%Xe gas mixtures. In section 2, the model is described by the quantities (β, α), which represent the percentage of the gas in the mixture. In
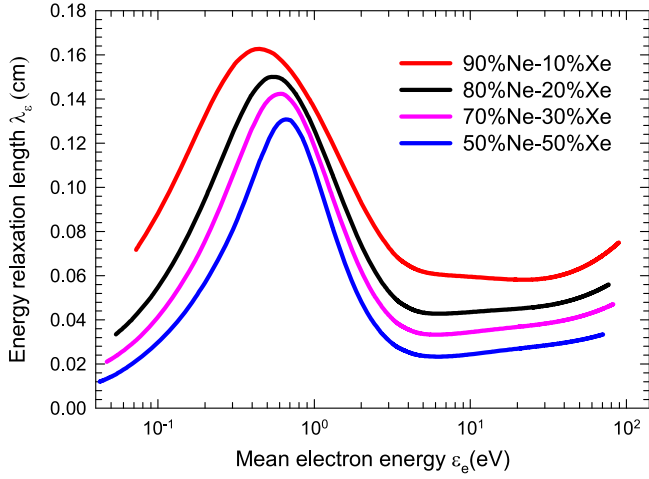
Figure 1. The energy relaxation length as a function of the mean electron energy for four mixtures at 1.5 Torr.
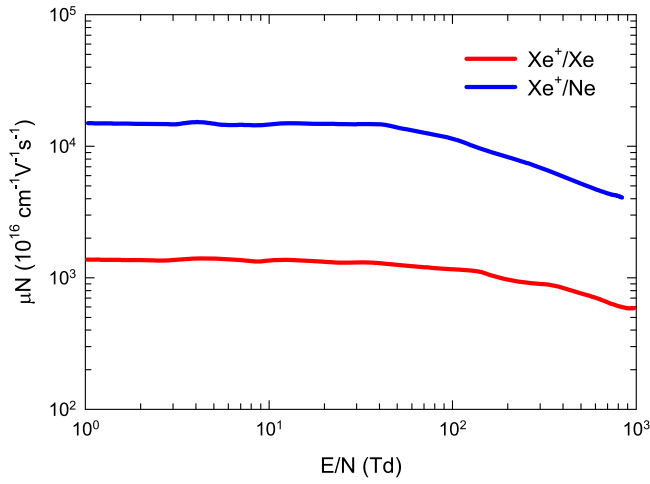

Figure 2. The mobilities of the positive ions of xenon in xenon and neon.

section 3, the results are discussed. Finally, a working conclusion is given in section 4.

2. Mathematical model

In order to validate the local EEDF assumption, which is used in this work, we are going to calculate the energy relaxation length as expressed as follows:

$$\lambda_\varepsilon = 2D_e\left(\nu_e + \frac{2m_e}{M_{Ne}}\nu_{Ne} + \frac{2m_e}{M_{Xe}}\nu_{Xe} + \nu_{Ne}^* + \nu_{Xe}^*\right)^{-0.5}$$
$$= 2D_e(\nu_t)^{-0.5}.$$

The total collision frequency (ν_t) and the electron diffusion coefficient (D_e) are calculated using BOLSIG+ software [14]. Figure 1 represents the energy relaxation length as a function of the mean electron energy for four gas mixtures. We remark that the energy relaxation length is less than the inter-electrode spacing (1 cm). This remark confirms our assumption of the local EEDF.

The chemical reactions intervening in the discharge are identical, as mentioned in [7]. Firstly, the process of the elastic collision of each gas intervenes in the discharge, and is described by the chemical reaction R1

$$A + e^- \rightarrow A + e^-, \tag{R1}$$

where A plays the role of both neon and xenon gas, and the coefficient P_{ec}^A related to this process is the energy loss per electron and is calculated according to [15]. Note that P_{ec}^A is in eVs^{-1} units. The ionization process is described by reaction R2

$$A + e^- \rightarrow A^+ + 2e^-, \tag{R2}$$
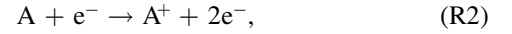
and the ionization coefficient of each gas is K_{io}^A, which depends on the mean electron energy and is calculated using BOLSIG+ software [14]. The excitation process is explained by reaction R3

$$A + e^- \rightarrow A_m^* + e^-, \tag{R3}$$
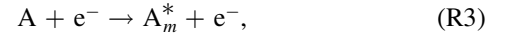
in which the subscript m is the metastable state of each gas. In this work, a metastable level of neon of $2p^53s$ was considered [16] and a $^3P_2$ level was considered for xenon [17]. The corresponding excitation coefficient is K_{ex}^A, and was determined by BOLISG + software [14]. The de-excitation process is defined according to reaction R4

$$A_m^* + e^- \rightarrow A + e^-, \tag{R4}$$
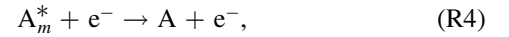
where the corresponding de-excitation coefficient is K_{dex}^A, and is calculated by BOLSIG+ software [14]. Note that K_{io}^A, K_{ex}^A and K_{dex}^A are in cm^3 s^{-1} units. The chemo-ionization process, which intervenes in our discharge, is defined by reaction R5

$$A_m^* + A_m^* \rightarrow A^+ + e^- + A, \tag{R5}$$

where the related chemo-ionization coefficient is K_{ci}^A, is taken from 4.8×10^{-10} cm^3 s^{-1} [17] of xenon and is equal to 3.6×10^{-10} cm^3 s^{-1} [18] of neon. The radiation process is defined as follows:

$$A_m^* \rightarrow A + h\nu, \tag{R6}$$

where ν is the absorbing photon frequency and h is the Plank's constant. By this reaction we can define the metastable lifetime of a gas as τ_m^A, which is equal to 2.7×10^6 s^{-1} of xenon [19] and takes about $2 \times 10^{-3}/p$ s with p in Torr of neon [16]. The stepwise ionization process in our discharge is described by the following reaction:

$$e^- + A_m^* \rightarrow A^+ + 2e^-, \tag{R7}$$
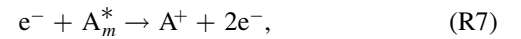
where the related coefficient of this reaction is named $K_{m\text{-}io}^A$ given in cm^3 s^{-1}, and is calculated from an analytical expression given by Vriens and Smeets [20]. Note that previous reactions implement neon and xenon too.

The latest chemical reaction as considered in our discharge is defined as follows:

$$Ne_m^* + Xe \rightarrow Xe^+ + e^- + Ne, \tag{R8}$$
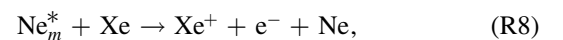
and the related coefficient is named as chemo-ionization-de-excitation—i.e. the chemo-ionization process of xenon and the de-excitation process of neon is labeled as K_{ci}^{NeXe} and is equal to 7.5×10^{-11} cm^3 s^{-1} [21]. Note that metastable Xe

Table 1. Description of the different notations utilized in our model.

Notations	Description	Notations	Description
n_e	Electron density	ε_{io}^{gas}	Energy loss of ionized atoms of a gas
n_+^{gas}	Positive ion density of a gas	ε_{ci}^{gas}	Energy gain of chemo-ionization processes of a gas
n_m^{gas}	Metastable atom density of a gas	ε_e	The mean electron energy
φ_+^{gas}	Positive ion flux of a gas	$\varphi_{e\varepsilon}$	The electron energy flux
φ_m^{gas}	Metastable atom flux of a gas	$S_{e\varepsilon}$	The source term of the energy equation
φ_e	Electron flux	τ_m^{gas}	The metastable lifetime of a gas
n_o	Constant background gas density	V	The electric potential
S_e	Electron source term	E	The electric field
S_+^{gas}	Positive ion source term of a gas	ε_o	The free space permittivity
S_m^{gas}	Metastable atom source term of a gas	e_o	The elementary charge
ε_m^{gas}	Energy loss of excited atoms of a gas	μ_e	The electron mobility
$\mu_{gas^+}^{mixture}$	The positive ion mobility of a gas in the mixture	$D_{gas^+}^{mixture}$	The positive ion diffusion coefficient of a gas in a mixture
D_e	The diffusion coefficient of electrons	α and β	The percentage of gas in the mixture
D_m^{gas}	The diffusion coefficient of metastable atoms of a gas	K_B	The Boltzmann constant
T	The gas mixture temperature	$D_{e\varepsilon}$	The diffusion coefficient of electron energy
$\mu_{e\varepsilon}$	The mobility of electron energy	M_{gas}	The atomic mass
m_e	The electron mass	ν_e	e−e collision frequency
ν_{gas}	Elastic e-atom collision frequency	ν_{gas}^*	Inelastic e−atom collision frequency
ν_t	Total collision frequency		

cannot ionize the Ne atom, because the energy of Xe_m^* is less than the energy of Ne^+.

The mathematical model is based on the first three moments of the Boltzmann equation, which are coupled with Poisson's equation; the metastable atom equation is also included in the model. Then, a description of the model is given by equations (1) to (25). Note that the difference between the existing model and the model given by [7, 8] is devoted to the presence of both α and β percentages of the gas as well as the positive ion mobility of each gas in the mixture. Table 1 represents a description of the different notations utilized in the present model.

$$\frac{\partial n_e}{\partial t} + \frac{\partial \varphi_e}{\partial x} = S_e, \tag{1}$$

$$\frac{\partial n_+^{Ne}}{\partial t} + \frac{\partial \varphi_+^{Ne}}{\partial x} = S_+^{Ne}, \tag{2}$$

$$\frac{\partial n_+^{Xe}}{\partial t} + \frac{\partial \varphi_+^{Xe}}{\partial x} = S_+^{Xe}, \tag{3}$$

$$\frac{\partial n_m^{Ne}}{\partial t} + \frac{\partial \varphi_m^{Ne}}{\partial x} = S_m^{Ne}, \tag{4}$$

$$\frac{\partial n_m^{Xe}}{\partial t} + \frac{\partial \varphi_m^{Xe}}{\partial x} = S_m^{Xe}, \tag{5}$$

$$S_+^{Ne} = n_e(\alpha n_o K_{o\_io}^{Ne} + n_m^{Ne} K_{m\_io}^{Ne}) + n_m^{Ne} n_m^{Ne} K_{ci}^{Ne}, \tag{6}$$

$$S_+^{Xe} = n_e(\beta n_o K_{io}^{Xe} + n_m^{Xe} K_{m\_io}^{Xe})$$
$$+ n_m^{Xe} n_m^{Xe} K_{ci}^{Xe} + \beta n_o n_m^{Ne} K_{ci}^{NeXe}, \tag{7}$$

$$S_e = S_+^{Ne} + S_+^{Xe}, \tag{8}$$

$$S_m^{Ne} = n_e(\alpha n_o K_{ex}^{Ne} - n_m^{Ne} K_{dex}^{Ne} - n_m^{Ne} K_{m\_io}^{Ne})$$
$$- 2n_m^{Ne} n_m^{Ne} K_{ci}^{Ne} - \frac{n_m^{Ne}}{\tau_m^{Ne}} - \beta n_o n_m^{Ne} K_{ci}^{NeXe}, \tag{9}$$

$$S_m^{Xe} = n_e(\beta n_o K_{ex}^{Xe} - n_m^{Xe} K_{dex}^{Xe} - n_m^{Xe} K_{m\_io}^{Xe})$$
$$- 2n_m^{Xe} n_m^{Xe} K_{ci}^{Xe} - \frac{n_m^{Xe}}{\tau_m^{Xe}}, \tag{10}$$

$$\frac{\partial \varepsilon_e n_e}{\partial t} + \frac{\partial \varphi_{e\varepsilon}}{\partial x} = S_{e\varepsilon}, \tag{11}$$

$$S_{e\varepsilon} = -e\varphi_e E + \varepsilon_m^{Xe} n_e n_m^{Xe} K_{dex}^{Xe} + \varepsilon_m^{Ne} n_e n_m^{Ne} K_{dex}^{Ne}$$
$$+ \varepsilon_{ci}^{Xe} n_m^{Xe} n_m^{Xe} K_{ci}^{Xe} + \varepsilon_{ci}^{Ne} n_m^{Ne} n_m^{Ne} K_{ci}^{Ne}$$
$$+ \varepsilon_{ci}^{NeXe} n_m^{Ne} \beta n_o K_{ci}^{NeXe} - n_e P_{ec}^{Xe} - n_e P_{ec}^{Ne}$$
$$- n_e(\varepsilon_m^{Xe} \beta n_o K_{ex}^{Xe} + \varepsilon_{io}^{Xe} \beta n_o K_{io}^{Xe}$$
$$+ (\varepsilon_{io}^{Xe} - \varepsilon_m^{Xe}) n_m^{Xe} K_{m\_io}^{Xe} + (\varepsilon_{io}^{Ne} - \varepsilon_m^{Ne}) n_m^{Ne} K_{m\_io}^{Ne}$$
$$+ \varepsilon_m^{Ne} \alpha n_o K_{ex}^{Ne} + \varepsilon_{io}^{Ne} \alpha n_o K_{io}^{Ne}), \tag{12}$$

$$\frac{\partial^2 V}{\partial x^2} = -\frac{e_o}{\varepsilon_o}(n_+^{Ne} + n_+^{Xe} - n_e), \tag{13}$$

$$\beta = 1 - \alpha, \tag{14}$$

$$\varepsilon_{ci}^{gas} = 2\varepsilon_m^{gas} - \varepsilon_{io}^{gas}. \tag{15}$$

The flux expressions of a particle are given as follows [22, 23]:

$$\varphi_e = -n_e \mu_e E - \frac{\partial D_e n_e}{\partial x}, \tag{16}$$

$$\varphi_+^{Ne} = n_+^{Ne} \mu_{Ne^+}^{NeXe} E - \frac{\partial D_{Ne^+}^{NeXe} n_+^{Ne}}{\partial x}, \tag{17}$$

$$\varphi_+^{Xe} = n_+^{Xe} \mu_{Xe^+}^{NeXe} E - \frac{\partial D_{Xe^+}^{NeXe} n_+^{Xe}}{\partial x}, \tag{18}$$

$$\varphi_m^{Ne} = -D_m^{Ne} \frac{\partial n_m^{Ne}}{\partial x}, \tag{19}$$

Table 2. The drift velocity and the mobility of a positive gas ion in the gas, where E/N is in Td, $a=420\,293\,012.8323$; $b=1.0921$ and $c=34\,565\,805.347\,398\,463$.

Gas	Drift velocity of positive neon ion in (m s^{-1})	Mobility of positive xenon ion
Neon	$w_{Ne^+}^{Ne} = (11.27E/n)/(1+0.01288E/n)^{0.5}$ [24]	Shown in figure 2 [26]
Xenon	$w_{Ne^+}^{Xe} = (aE/n)^b/(c^b + (E/n)^b)$	Shown in figure 2 [26]

$$\varphi_m^{Xe} = -D_m^{Xe}\frac{\partial n_m^{Xe}}{\partial x}, \qquad (20)$$

$$\varphi_{e\varepsilon} = -n_e E \mu_{e\varepsilon} - \frac{\partial n_e D_{e\varepsilon}}{\partial x}, \qquad (21)$$

$$\frac{1}{\mu_{gas1^+}^{mixture}} = \frac{\alpha}{\mu_{gas1^+}^{gas1}} + \frac{\beta}{\mu_{gas1^+}^{gas2}}, \qquad (22)$$

$$D_{gas^+}^{mixture} = \frac{\mu_{gas^+}^{mixture} T K_B}{e_o}, \qquad (23)$$

$$D_{e\varepsilon} = \frac{5 D_e \varepsilon_e}{3}, \qquad (24)$$

$$\mu_{e\varepsilon} = \frac{5 \mu_e \varepsilon_e}{3}. \qquad (25)$$

Figure 3. Current–voltage characteristics in 90%Ne-10%Xe, 80% Ne-20%Xe, 70%Ne-30%Xe and 50%Ne-50%Xe gas mixtures, with $T_1 = 7 \times 10^{-5}$ s, $T_2 = 3.6 \times 10^{-5}$ s and $T_3 = 6 \times 10^{-5}$ s, which each represent the maximum time of the simulation, and also represent the steady state of the discharge.

The gas ion mobility in the mixture is determined according to equation (22). Table 2 represents the drift velocity and the mobility of a positive gas ion in the gas. $W_{Ne^+}^{Ne}$ is given by a mathematic expression as a function of the reduced electric field by Frost [24]. $W_{Ne^+}^{Xe}$ is developed according to the results given by Piscitelli *et al* [25]. Equation (23) is used to calculate the positive ion diffusion coefficient of a gas in the mixture. Note that the parameter transport of electrons in the Ne-Xe mixture changed for each (β, α) value, and was calculated by BOLSIG+ software [14]. The geometry of the electrodes used in this work is similar to that in paper [7].

3. Results and discussion

Figure 3 represents the current–voltage characteristics in the 90%Ne-10%Xe, 80%Ne-20%Xe, 70%Ne-30%Xe and 50% Ne-50%Xe gas mixture glow discharges at low pressure. The inter-electrode spacing is taken as constant and is equal to 1 cm. The gas temperature is equal to 300 K, and the pressure is taken as equal to 1.5 Torr. The secondary electron emission coefficient is supposed to be constant, is equal to 0.26 for positive neon ions [1] and equal to 0.03 for positive xenon ions [27]. Note that all points in figure 3 are taken from the spatial distributions of the current densities, which are strictly constant in all space in the inter-electrode, i.e. variable spatial distributions of current densities are not considered. Also note that these distributions are taken in the stationary state of the discharge. The stationary state of the discharge depends on the applied potential of the electrodes and the percentage (β, α) values in the mixture. For example, the point (30%Xe, 150 V) converges at $T_1 = 7 \times 10^{-5}$ s, and the point (30%Xe, 500 V) converges at $T_2 = 3.6 \times 10^{-5}$ s. We remark that the
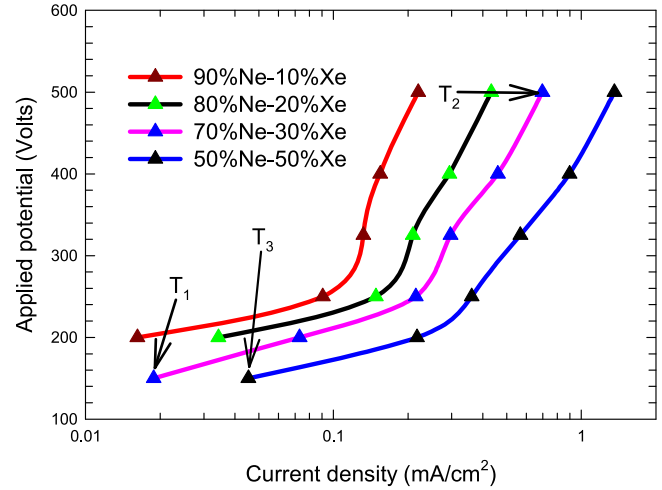
electric potential accelerates the convergence of the discharge. The point (50%Xe, 150 V) converges at $T_3 = 6 \times 10^{-5}$ s. We now remark that the percentage of xenon accelerates the convergence of the discharge, i.e. for a growth value of β the steady state of the discharge becomes short in duration. In order to examine these curves (figure 3), we remark that they are characterized by two modes, i.e. the normal and abnormal glow discharge modes. For example, the abnormal glow discharge mode is defined in the range (superior than 300 V) in the 90%Ne-10%Xe gas mixture, and is defined in the range (superior than 200 V) in the 50%Ne-50%Xe gas mixture. These curves are the same as those obtained in several experimental studies of pure gases. Note that the spatial distribution of the xenon ion density is important for the neon ion density, despite the presence of an important percentage of neon in the mixture, and the neon ion density is negligible compared to the xenon ion density for an elevated percentage of xenon in the mixture. This is due to the threshold ionization of each gas, in which the threshold ionization of xenon is less than the threshold ionization of neon. This phenomenon is also observed in paper [7]. To conclude, the current–voltage characteristics in the 90%Ne-10%Xe, 80%Ne-20% Xe, 70%Ne-30%Xe and 50%Ne-50%Xe gas mixtures are well defined by the two modes of the discharge. But, for the well-defined normal glow discharge mode, it is necessary for the simulation to take a long time.
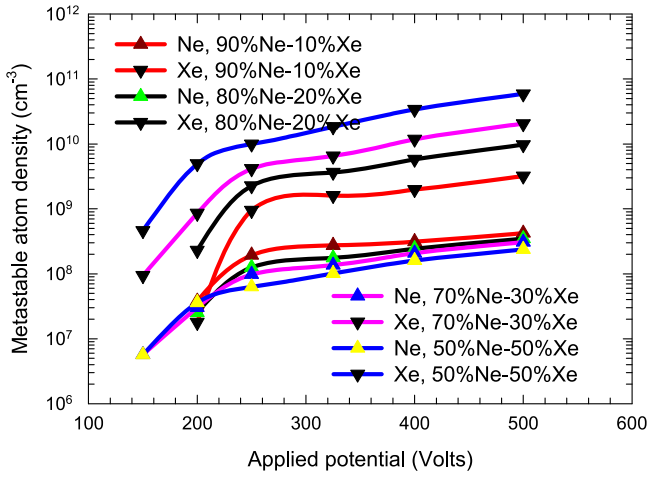
Figure 4. The maximum values of the metastable neon and xenon atom densities as a function of the electric potential in 90%Ne-10%Xe, 80%Ne-20%Xe, 70%Ne-30%Xe and 50%Ne-50%Xe gas mixtures at a pressure of 1.5 Torr.

Figure 5. The electric field at the cathode as a function of the electric potential in the 90%Ne-10%Xe, 80%Ne-20%Xe, 70%Ne-30%Xe and 50%Ne-50%Xe gas mixtures at a pressure of 1.5 Torr.

Figure 4 represents the maximum values of the neon and xenon metastable atom densities as a function of the electric potential in the 90%Ne-10%Xe, 80%Ne-20%Xe, 70%Ne-30%Xe and 50%Ne-50%Xe gas mixtures at a pressure of 1.5 Torr. We note that the metastable xenon atom density is superior to the metastable neon atom density due to the threshold excitation of each gas, in which the threshold excitation of xenon is less than the threshold excitation of neon. We remark that the percentage (β, α) of gas in the mixture as well as the applying voltage are highly consequent on the metastable atom densities, which increase with the electric potential. This is due to the augmentation of the electric field, which causes a lot of excitation collisions. We note that both the curves of the neon and xenon metastable atom densities are separate in the range of the applied voltage, mostly in the percentage of neon gas inferior to 90%.

Figure 5 represents the electric field at the cathode as a function of the electric potential in the 90%Ne-10%Xe, 80%
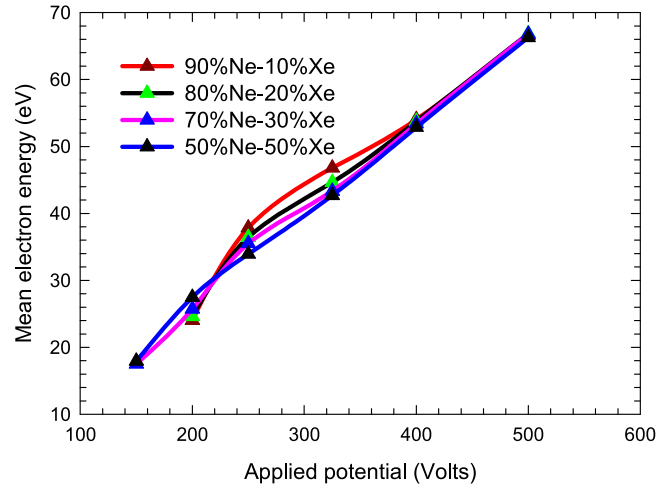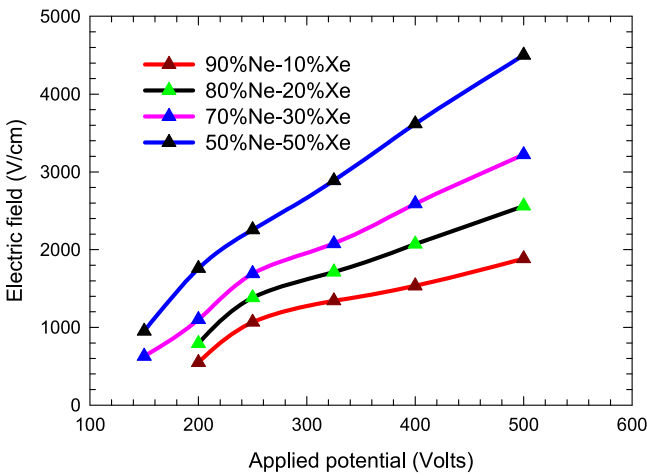

Figure 6. The maximum values of the mean electron energy as a function of the electric potential in the 90%Ne-10%Xe, 80%Ne-20%Xe, 70%Ne-30%Xe and 50%Ne-50%Xe gas mixtures at a pressure of 1.5 Torr.

Ne-20%Xe, 70%Ne-30%Xe and 50%Ne-50%Xe gas mixtures at a pressure of 1.5 Torr. We observe that the electric field increases with the augmentation of the electric potential; this is clearly evident when we utilize the formulation of the gradient of the electric potential. Note that the electric field increases with the percentage of xenon gas due to the threshold ionization.

Figure 6 represents the maximum values of the mean electron energy as a function of the electric potential in the 90%Ne-10%Xe, 80%Ne-20%Xe, 70%Ne-30%Xe and 50% Ne-50%Xe gas mixtures at a pressure of 1.5 Torr. We note that the effect of the percentage (β, α) of the gas in the mixture is negligible in the range (>400 V). This is due to the value of the potential, which is sufficient to ionize each gas. In view of this figure, we conclude an important remark, namely that the mean electron energy decreases with an increase of the percentage of xenon (β) for a range of voltages, and the mean electron energy increases with the increase of the percentage of xenon for another range of voltages. As an example for the range (>250 V), we remark that the mean electron energy in the 90%Ne-10%Xe gas mixture is superior to the mean electron energy in the 50%Ne-50%Xe gas mixture. Furthermore, for the range (<250 V), the mean electron energy in the 50%Ne-50%Xe gas mixture is superior to the mean electron energy in the 70%Ne-30%Xe gas mixture. These observations are related to the type of glow discharge mode, i.e. in the normal glow discharge mode, the mean electron energy increases with the percentage β, and in the abnormal glow discharge mode the mean electron energy decreases with the augmentation of the percentage β.

4. Conclusion

By applying the fluid model method, we have identified the normal and abnormal glow discharge modes in 90%Ne-10% Xe, 80%Ne-20%Xe, 70%Ne-30%Xe and 50%Ne-50%Xe gas

mixtures at a pressure of 1.5 Torr. The results show that the mean electron energy increases with the increase of the percentage of xenon gas in the mixture in the normal glow discharge mode. In the abnormal glow discharge mode, the mean electron energy decreases with the increase of the percentage of the xenon gas in the mixture. Finally, these results present a range of references in the literature, which will help to ameliorate the present model in the future.

References

[1] Chapman B N 1980 *Glow Discharge Processes* (New York: Wiley)

[2] Harrison W W 1988 *Glow Discharge Mass Spectrometry* (New York: Wiley)

[3] Marcus R K 1993 *Glow Discharge Spectroscopies* (New York: Plenum Press)

[4] Meyyappan M and Kreskovsky J P L 1990 *J. Appl. Phys.* **68** 1506

[5] Bogarets A, Gijbels R and Goedheer W J 1995 *J. Appl. Phys.* **78** 2233

[6] Bouchikhi A and Hamid A 2010 *Plasma Sci. Technol.* **12** 59

[7] Bouchikhi A 2017 *Plasma Sci. Technol.* **19** 095403

[8] Bouchikhi A 2018 *Can. J. Phys.* **96** 62

[9] Kolobov V I and Godyak V A 1995 *IEEE Trans. Plasma Sci.* **23** 503

[10] Zhu X M *et al* 2012 *Plasma Sources Sci. Technol.* **21** 024003

[11] Wei W, Sun J and Guo B 2007 *Eur. Phys. J. Appl. Phys.* **37** 331

[12] Panchenko A N *et al* 1999 *Russ. Phys. J* **42** 557

[13] Hassouba M A and Mehanna E A 2009 *Int. J. Phys. Sci* **4** 713

[14] Hagelaar G J M and Pitchford L C 2005 *Plasma Sources Sci. Technol.* **14** 722

[15] Van Gaens W and Bogaerts A 2014 *J. Phys. D Appl. Phys.* **47** 079502

[16] Pike E W 1936 *Phys. Rev.* **49** 513

[17] Kolokolov N B, Kudrjavtsev A A and Blagoev A B 1994 *Phys. Scr.* **50** 371

[18] Sheverev V A, Stepaniuk V P and Lister G G 2002 *J. Appl. Phys.* **92** 3454

[19] Galy J *et al* 1993 *J. Phys.* B **26** 447

[20] Vriens L and Smeets A H M 1980 *Phys. Rev.* A **22** 940

[21] Levin L A *et al* 1981 *IEEE J. Quantum Electron.* **17** 2282

[22] Becker M M, Loffhagen D and Schmidt W 2009 *Comput. Phys. Commun.* **180** 1230

[23] Alili T, Bouchikhi A and Rizouga M 2016 *Can. J. Phys.* **94** 731

[24] Frost L S 1957 *Phys. Rev.* **105** 354

[25] Piscitelli D *et al* 2003 *Phys. Rev.* E **68** 046408

[26] Meunier J, Belenguer P and Boeuf J P 1995 *J. Appl. Phys.* **78** 731

[27] Almeida P G C, Benilov M S and Faria M J 2010 *Plasma Sources Sci. Technol.* **19** 025019